DIELECTRIC SPECTROSCOPIC ANALYSIS OF $La_{0.75}Ba_{0.25}Fe_{1-X}CO_XO_3$($X$ = 0.0, 0.05, 0.1, 0.15, 0.20, 0.30)

J. Ahmad[1*], W. Javed[1], S. H. Bukhari[2], U. Nissar[1], J.A. Khan[1], H. Abbas[1], T. Sultan[3] and A. Latif[3]

[1]Department of Physics, Bahauddin Zakariya University, Multan 6800, Pakistan.
[2]Department of Physics, G.C. University Faisalabad, Sub-Campus, 31200 Layyah, Pakistan.
[3]Department of Civil Engineering, Bahauddin Zakariya University, Multan 60800, Pakistan.
[*]Corresponding Author Email: javedahmad@bzu.edu.pk, dr.j.ahmad@gmail.com

ABSTRACT: Single phase nano crystalline powder of $La_{0.75}Ba_{0.25}Fe_{1-x}Co_xO_3$ for x ranging from 0.0-0.3 has been prepared using sol-gel method. For dielectric measurements, a steep decrease in the dielectric constant and dielectric has been observed in low frequency region, which tends to show no change at high frequency suggesting a usual dielectric dispersion. The observed dielectric dispersion behavior is directly related to the dipole moments produced due to mobility of localized charge carriers. The impedance measurements are used to show the grain boundary effects. Cole-Cole plot and frequency dependent conductivity measurements clearly demonstrate the conductive behavior of the ceramics.

Key words: X-ray Diffraction; Dielectric constant; Perovskite; Impedance

(Received 03.01.2021 Accepted 23.03.2021)

INTRODUCTION

Perovskite oxides with a general formula ABO_3 where A&B represent lanthanides and transition metals respectively, are considered potential candidates for technological applications such as oxygen permeable membranes, fuel cell electrodes and oxygen catalysts (Mawdsley & Krause, 2008). Such applications are mainly due to variety of properties they exhibit due to their complex structural features. $LaFeO_3$ is orthorhombic and behaves as an anti-ferromagnet insulator at room temperature. It is known that if Fe is substituted with Co, the resulted material i.e., $LaCoO_3$ with increased ionic conductivity possesses great potential for technological applications (Chern, Hsieh, Tai, & Hsung, 1998; Kemik, Takamura, & Navrotsky, 2011). In this article $La_{0.75}Ba_{0.25}Fe_{1-x}Co_xO_3$ (x=0.0-0.3) were synthesized by sol gel method. The major goal was to study the effect of doping of Co concentrations. The amount of Co concentration is crucial for metal-insulator (MI) transition because for Co between 0.1 and 0.15, a remarkable indication of the MI transition has been found. Such ABO_3 oxides demonstrate remarkable ferroelectric response. It is expected that the high dielectric polarization existed may be due to metallic phase (Jonker & Van Santen, 1953; Sarma, 1988). The higher dielectric constant at low frequency is associated with the charge carriers which are free. Thus, the synthesized samples are characterized by different experimental techniques in order to study the dielectric properties of these perovskites.

MATERIALS AND METHODS

Barium and Cobalt substituted oxides $La_{0.75}Ba_{0.25}Fe_{1-x}Co_xO_3$ (LBFCO) for x ranging from 0.0-0.3 have been prepared by wet chemical usual sol gel technique. The reagent grade cobalt nitrate, iron nitrate, lanthanum nitrate, barium nitrate, all in hydrous form, and citric acid were taken in stoichiometric ratio, mixed in deionized water to form a solution and citric acid was added. Then it was heated at 70^0C stirring it continuously in order to evaporate the solution. During this process the pH=7 was maintained with the addition of Ammonia drop-wise. The color of the product was continuously observed during the heating process until it became dark brown. This evaporation process took 22 hours for the solution to turn into gel form and further 1 hour to change into powder form. The whole process can be chemically demonstrated by the following equation;

$$[Ba(NO_{3)2}]_{0.25} + [Fe(NO_3)_3.9H_2O]_{1-} + [La(NO_3)_3.6H_2O]_{\mathbf{0.75x}} + [Co(NO_3)_2.6H_2O]_x + C_6H_8O_7.H_2O + NH_3.H_2O = [La_{0.75}Ba_{0.25}Fe_{1-x}Co_xO_3] + CO_2 + N_2 + H_2O \quad (1)$$

where x has the value as 0.0, 0.05, 0.1, 0.15, 0.20, 0.30. The obtained powder was grinded for 30 minutes using agate mortar and pestle and sintered at 800˚C for 6 hours. The powder was pressed with the help of a hydraulic press to make small pellets having a diameter of 7mm. These pellets were used to study the structural and dielectric properties. The dielectric properties were measured by using the LCR meter (HP 4192A).

RESULTS AND DISCUSSIONS

The XRD pattern of the prepared LBFCO for x ranging from 0.0-0.3 nano crystalline materials has been shown in Fig. 1. All main XRD peaks have been indexed and thus found no un-indexed peak which is an indication of single phase of the synthesized materials. The crystalline nature of the materials is evident from the well-defined peaks at different angles and all doped samples exhibit quite similar pattern as the $LaFeO_3$. This reflects that the doping of Co ions in place of Fe and Ba ions in place of La site does not change the peak position and thus the structure of the system almost remains the same. This suggests no prominent distortion in perovskite structure of LBFO taken place with the doping of Co. Moreover, the intensity of the diffracted peaks for Co doped samples is smaller as compared to the undoped LBFO (Ge, Liu, & Liu, 2001; Li *et al*., 2011) The structure of $La_{0.75}Ba_{0.25}Fe_{1-x}Co_xO_3$ is orthorhombic and the constants can be determined with the help of Miller indices and by using the following equation

$$Sin^2\Theta=Ah^2+Bk^2+Cl^2 \quad (2)$$

The values of A, B and C can be calculated by using the following relations $A = \lambda^2/4a^2$, $B = \lambda^2/4b^2$ and $C = \lambda^2/4c^2$, respectively.

The following Scherer formula has been employed to determine the crystallite size

$$D = K.\lambda / \beta.Cos\theta \quad (3)$$

where K = 0.98 and λ, θ, β are respectively the wavelength of Cu K_α= (1.5406 Å), the Bragg's angle, and the full width at half maximum. The crystallite size is found to increase with the dopant Co^{2+} because of the greater radius of Co^{2+} shown in Fig. 2. The cell volume is found to increase when Ba^{2+} is doped in pure $LaFeO_3$. Assuming orthorhombic structure, all observed diffraction peaks were indexed. This suggests that La^{3+} has been partially substituted by Ba^{2+} without altering the crystal structure and therefore, an increase in volume of the unit cell is expected owing to the larger ionic radius of Ba^{2+} (135 pm) as compared to La^{3+} (106.1 pm) (Song *et al*., 2005) ; but after the Co^{2+} doping in place of Fe^{3+} the volume increases at first then decreases as the dopant concentration increases. The increase may be due to the fact that the Co^{2+} radius (0.74Å) is bigger as compared to Fe^{3+} (0.64Å). If Fe^{3+} ions are partially substituted with Co^{2+} ions (Akgul, Ergin, Sekerci, & Atici, 2007), the decrease in volume with increase in construction can be due to formation of Co^{3+} (53 pm) produced due to oxidization of Co^{2+} ions (Sun, Qin, Wang, Zhao, & Hu, 2011). X-ray density can be calculated by using the relation.

$$d_x = Z.M / N_A V_{cell} \quad (4)$$

Where Z, M, N_A, V_{cell} symbols are for the no. of formula units, formula mass, Avogadro's no. and unit cell volume, respectively. As the structure is orthorhombic the value of Z = 4 (Ge *et al*., 2001). The trend of X-ray density is in accordance with the volume of the samples as explained earlier that is depicted in Fig. 3. Bulk density is calculated as

$$d_b = m / V \quad (5)$$

where m and V represent mass and volume of the pellet respectively. The bulk density (d_b) and x-ray density (d_x) have been extracted from the XRD pattern which has been utilized to calculate the porosity (P) using the relation;

$$P = (1-d_b/d_x).100 \quad (6)$$

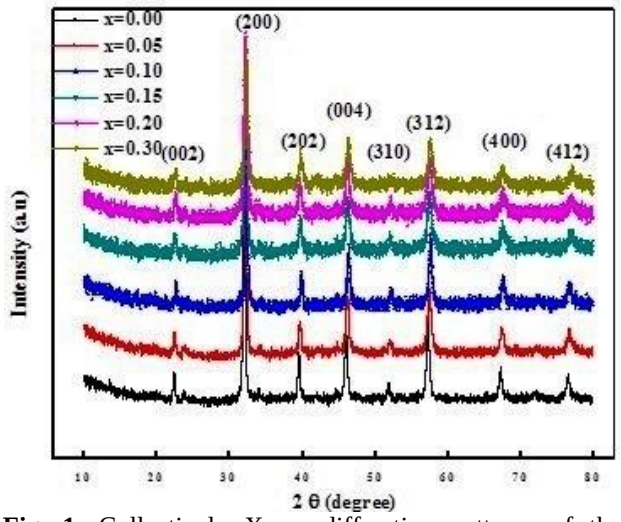

Fig. 1. Collectively X-ray diffraction patterns of the LBFCO for x ranging from 0.0-0.3.

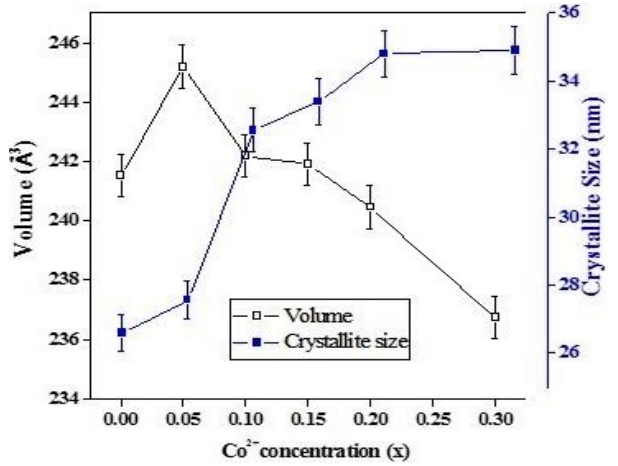

Fig. 2. Effect of Co concentration on the unit cell volume and crystallite size (nm).

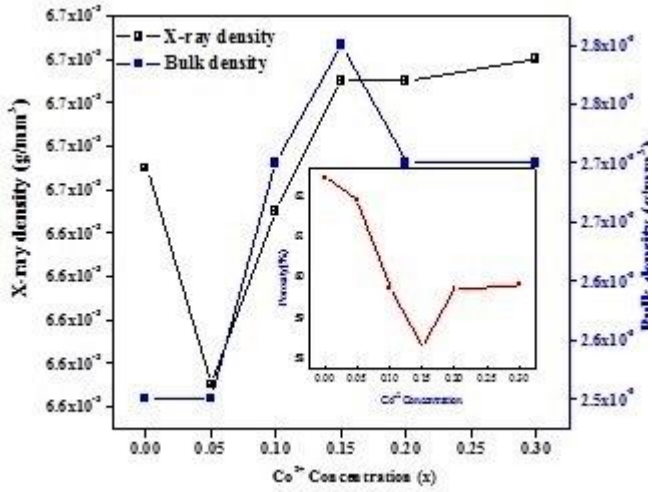

Fig. 3. Effect of Co^{2+} concentration on the X-ray density, Bulk density and Inset shows the Porosity (%).

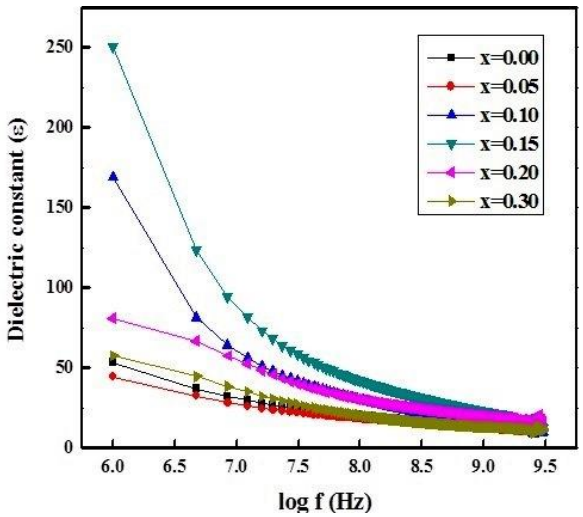

Fig. 4. Dielectric constant vs. log f (Hz).

Fig. 4 shows frequency dependent dielectric constant (ε) for $La_{0.75}Ba_{0.25}Fe_{1-x}Co_xO_3$ material at x = 0.0 in the frequency range 1MHz to 3GHz. The values of ε decrease with increasing frequency, which indicates that sample has usual dielectric dispersion behavior. The reason is that at high frequencies dipoles do not follow the alternating electric field so value of the ε becomes constant in this frequency range while at low frequencies dipoles follow the alternating electric field and all types of polarization are present. However, in present work we suggest that the high value of the ε in low frequencies range is due to ionic and interfacial polarization. At low frequency, the charges and its dipoles have enough time to align themselves in the direction of the applied external field resulting in pronounced 'ε' as happened in case of Maxwell Wagner polarization and interfacial polarization. Contrary to behavior of the dipoles for low frequency field, they fail to have enough time to re-align themselves in the direction of the field for high frequency and consequently the value of the ε drops down. The charge compensation process occurs due to comparable valence charges as La ions in $LaFeO_3$ are replaced with Ba ions. Further, in order to neutralize the total charge Fe ions are formed. The excess of Fe^{4+} ions instead of Fe^{3+} ions provides extra holes to the system thereby increasing the p-type charge carriers. These p-type charge carriers create dipoles that align themselves in the direction of externally applied electric field and thus a net polarization is contributed into the polarization present due to n-type charge carriers (Ahmad & Anwar, 2012; Bhadra, Al-Thani, Madi, & Al-Maadeed, 2017). It is also found that value of ε for $Ba_{0.25}La_{0.75}FeO_3$ sample is 55 at ~ 10^6 Hz. The value of ε changes with the dopant Co^{2+} but at the high frequency range the fluctuation in value is negligible small.

Fig. 5 demonstrates the relation of imaginary part of the ε with change in frequency. The imaginary part of the ε exhibits quite similar behavior as that of real part of the ε. In the present work, the samples for x = 0.10, 0.15 have high value of the imaginary part of the ε as compared to the ones for x = 0.00, 0.05. The complex impedance (Z) of the samples has also been measured at room temperature; real part of Z vs. imaginary part of Z are plotted as a cole-cole plot as shown in **Fig. 6.** As predicted theoretically, the Cole –Cole plot usually shows a semi-circle for high frequency region and almost a linear behavior for the low frequency region. For x=0.00 and x=0.05, we have the larger semicircle amongst all taken concentrations. Such behavior indicates high value of resistance offered by the interfacial charge transfer and also dictates the materials offer poor conductivity. On the other hand the cole-cole plot for the samples for x= 0.10, 0.15 possess smaller semi-circle radii. These later samples seem to offer low resistance (Lily, Prasad, & Choudhary, 2008). It is found that variation of grain boundary resistance is more dominant than the variation of grain resistance. This may be due to the existence of dangling bonds and also due to oxygen distributed non-stoichiometrically in the grain boundary regions that behave as a potential trap for the carriers which cannot move freely (Idrees *et al*., 2011). It can be seen from Fig. 7, high value have been observed for x=0.0 due to presence of defects and p–type carriers while at x= 0.05 concentration sample becomes more resistive because symmetry of structure is disturbed when Co^{2+} is doped in the sample initially. But on the increase of doping concentration like Co^{2+} defects and p-type carriers are removed and resistivity of the sample is decreased up to x = 0.15. For higher concentration of Co^{2+} doping, defects are increased which increases the resistivity of sample. It is reported that linear response in Z'' represents that sample has insulating behavior while semicircle plot

represents that sample has conducting behavior (Rao, Prasad, Krishna, Tilak, & Varadarajulu, 2006). Further it is found that terminal sample has low value of resistivity as compared to parent sample.

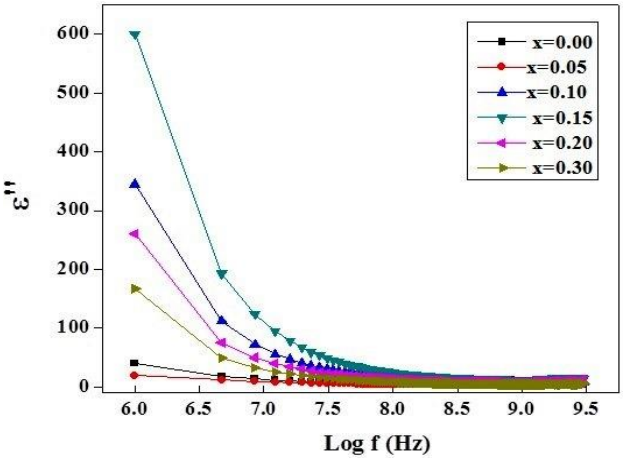

Fig. 5: Dielectric loss vs. log f (Hz).

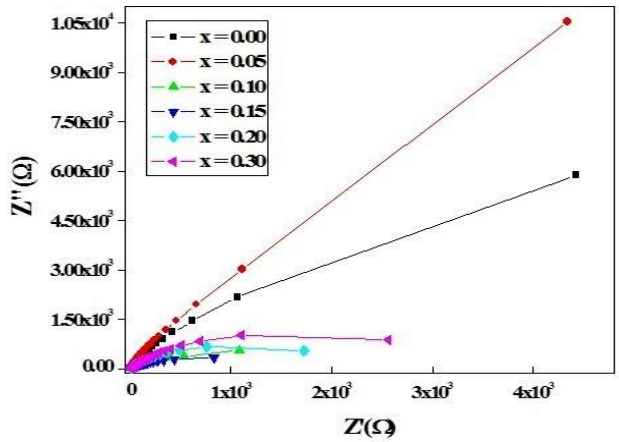

Fig. 6: Cole-Cole plots of in $La_{0.75}Ba_{0.25}Fe_{1-x}Co_xO_3$.

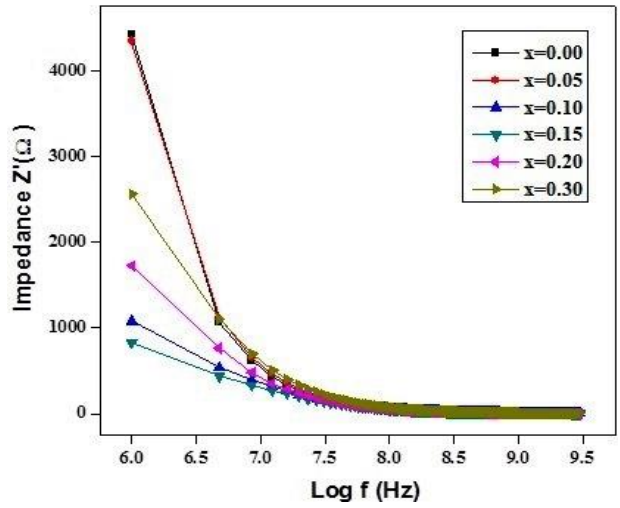

Fig. 7: Real part of impedance versus log f (Hz).

In Fig. 8, the behavior of Z' as a function of frequency has been shown for samples of various concentrations. The similar trend is observed as in case of real part of impedance. The same trend is already reported by N. Tawichai *et al*. (Tawichai *et al*., 2012). The variation in tangent loss (tanδ) is depicted in Fig. 9. The tanδ decreases with the increase of frequency indicating the effect of electrode polarization. Further, it is reported that variation of tanδ with frequency is same as the variation of the ε as observed in previous work [19]. The loss peaks are observed at the high frequency which indicates that the hopping of the charge carriers becomes exactly equal to the applied electric field. The reciprocal of the tanδ i.e. the quality factor 'Q' is displayed in Fig. 10. The maximum Q value suggests application of the materials in electronic devices (Murtazaab & Ahmad, 2016).

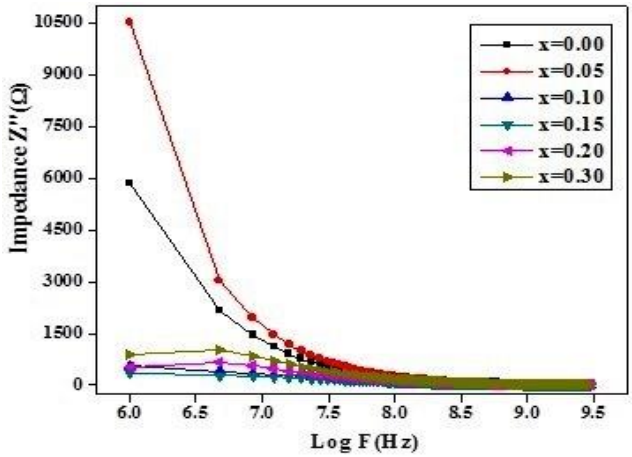

Fig. 8: Variation of imaginary part vs. log f (Hz).

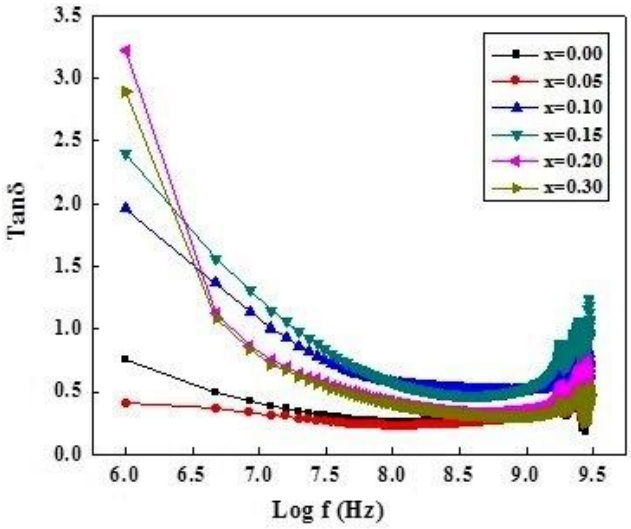

Fig. 9: Change in Tan δ as a function of log f (Hz).

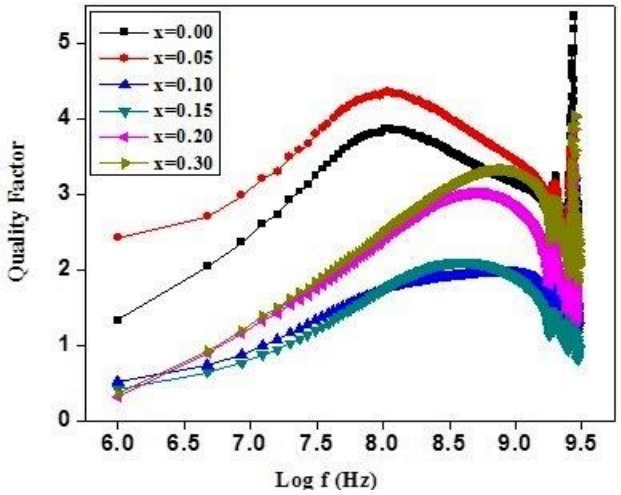

Fig. 10: Quality factor vs. log f (Hz).

Fig. 11 shows frequency dependence of conductivity for different concentrations. It can be seen from Fig. 11 that the sample (x = 0.15) shows high conductivity as compared to other samples. It is reported by X. Ge *et al*. (Ge *et al*., 2001) that defects are produced in the present system by increasing the concentration of Co^{2+} dopant beyond a certain limit which reduce the conductivity of the sample because defects cause obstruction in flow of charge carriers. Hence the present result indicates conductivity of our terminal compound drops due to increase in defects. Frequency dependence of ac conductivity σ (ω) follows the relation (Ramesan, 2012).

$$\sigma(\omega) = A\omega^{n} \quad (8)$$

'ω' the angular frequency; n the dimensionless exponent and A is the dimension of $\Omega^{-1}cm^{-1}$. The 'ε' and σ_{ac} are closely interconnected as reported in literature (Zhang & Fredkin, 1999).

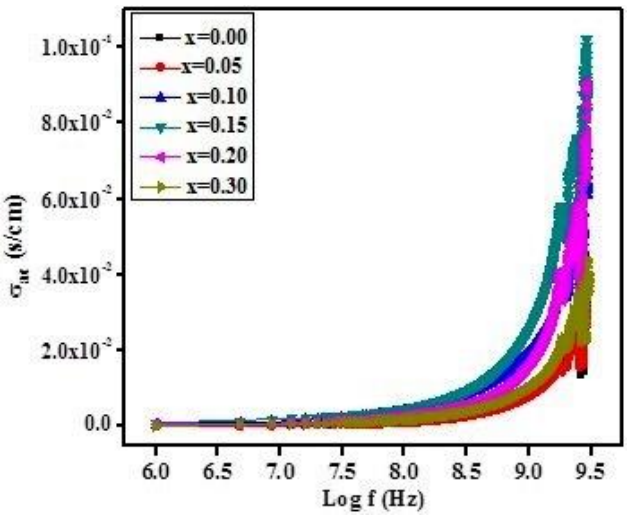

Fig. 11: Conductivity vs. log f (Hz).

Conclusions: The fine crystalline perovskite type multiferroics LBFCO for various composition of Co have been successfully synthesized by sol gel method and characterized in detail. In Structural properties**,** it has been concluded that the pure phase of the samples were formed at 800 ˚C. The particle size was found to increase due to doping of Co^{2+}. The volume of the sample increases when Ba^{2+} and Co^{2+} are added. The exactly opposite trend for the X-ray density was observed. Bulk density was found to increases in the beginning then decrease with the excess of Co^{+2} concentrations which reflects the presence of voids and cracks. The porosity percentage showed opposite behavior as that of bulk density. In Dielectric properties, steep decrease in the 'ε' as well as the Tan δ is attributed to dielectric dispersion usually observed in perovskite oxides and explained by Maxwell-Wagner Model. It is found that dielectric constant increases in the beginning due to Co^{+2} doping and in the final sample decreases and becomes same as the parent sample. The behavior of imaginary part of dielectric constant and loss tangent is also the same as that of dielectric constant. The trend is due to the doping of Co^{2+} which increases the hole concentration, when electric field is applied these excess carriers easily transport through good material i.e., grains. But at bad regions the carriers accumulate resulting a large polarization and high value of ε at low frequency. Moreover, these carriers do not follow the applied electric field for high frequencies. The decrease in the dielectric constant of the last sample (x=0.3) may be due to the increasing tendency of disorientation of the dipoles with the excess Co^{2+} concentration. Impedance analysis shows that the effect of grain boundaries is more dominant then the effects of grains. We found impedance change in the lower frequency region only which is actually due the grain boundary region. According the cole-cole plot the terminal compound is found to be less resistive as compared to the parent sample and in other words we can conclude that the compound LBFCO is more conductive as compared to parent sample. This behavior is also supported by the results of ac conductivity. The highest value of conductivity was found at the concentration x=0.15 because of the shortage of % porosity and it decreases afterwards due to increase of % porosity or it may be due to the presence of excess voids or defects in the material.

Acknowledgement: The financial support of the HEC, Pakistan through its NRPU No. 9301/ Punjab/ NRPU/ R&D/HEC/2017 is greatly acknowledged.

REFERENCES

Ahmad, J., & Anwar, S. (2012). Dielectric properties for the ordered-perovskite cuprate $Sr_2Cu(Re_{0.69}Ca_{0.31})O_6$. *Physica B: Condensed Matter, 407*(3), 412-415.

Akgul, U., Ergin, Z., Sekerci, M., & Atici, Y. (2007). AC conductivity and dielectric behavior of [Cd $(phen)_2$ $(SCN)_2$]. *Vacuum, 82*(3), 340-345.

Bhadra, J., Al-Thani, N. J., Madi, N. K., & Al-Maadeed, M. A. (2017). Effects of aniline concentrations on the electrical and mechanical properties of polyaniline polyvinyl alcohol blends. *Arabian journal of chemistry, 10*(5), 664-672.

Chern, G., Hsieh, W. K., Tai, M. F., & Hsung, K. S. (1998). High dielectric permittivity and hole-doping effect in La_{1-x} Sr_xFeO_3. *Physical Review B, 58*(3), 1252.

Ge, X., Liu, Y., & Liu, X. (2001). Preparation and gas-sensitive properties of $LaFe_{1-y}Co_yO_3$ semiconducting materials. *Sensors and Actuators B: Chemical, 79*(2-3), 171-174.

Idrees, M., Nadeem, M., Atif, M., Siddique, M., Mehmood, M., & Hassan, M. M. (2011). Origin of colossal dielectric response in $LaFeO_3$. *Acta Materialia, 59*(4), 1338-1345.

Jonker, G. H., & Van Santen, J. H. (1953). Magnetic compounds wtth perovskite structure III. ferromagnetic compounds of cobalt. *Physica, 19*(1-12), 120-130.

Kemik, N., Takamura, Y., & Navrotsky, A. (2011). Thermochemistry of $La_{0.7}Sr_{0.3}Mn_{1-x}Fe_xO_3$ solid solutions (0< x< 1). *Journal of Solid State Chemistry, 184*(8), 2118-2123.

Li, F.-t., Liu, Y., Sun, Z.-m., Liu, R.-h., Kou, C.-g., Zhao, Y., & Zhao, D.-s. (2011). Facile preparation of porous $LaFeO_3$ nanomaterial by self-combustion of ionic liquids. *Materials letters, 65*(2), 406-408.

Lily, K., Prasad, K., & Choudhary, R. N. P. (2008). Impedance spectroscopy of $(Na_{0.5}Bi_{0.5})(Zr_{0.25}Ti_{0.75})O_3$ lead-free ceramic. *J. Alloys Compd., 453*(1), 325-331.

Mawdsley, J. R., & Krause, T. R. (2008). Rare earth-first-row transition metal perovskites as catalysts for the autothermal reforming of hydrocarbon fuels to generate hydrogen. *Applied Catalysis A: General, 334*(1-2), 311-320.

Murtazaab, G., & Ahmad, I. (2016). SYNTHESIS, STUDY OF ELECTRICAL, THERMAL BEHAVIOR OF POLYANILINE-POLYSTYRENE SULPHONIC ACID COMPOSITE. *Digest Journal of Nanomaterials and Biostructures, 11*(4), 1261-1269.

Ramesan, M. T. (2012). In situ synthesis, characterization and conductivity of copper sulphide/polypyrrole/polyvinyl alcohol blend nanocomposite. *Polymer-Plastics Technology and Engineering, 51*(12), 1223-1229.

Rao, K. S., Prasad, D. M., Krishna, P. M., Tilak, B., & Varadarajulu, K. C. (2006). Impedance and modulus spectroscopy studies on $Ba_{0.1}Sr_{0.81}La_{0.06}Bi_2Nb_2O_9$ ceramic. *Materials Science and Engineering: B, 133*(1-3), 141-150.

Sarma, D. D. (1988). Electronic structure of high-T c superconductors from core-level spectroscopies. *Physical Review B, 37*(13), 7948.

Song, P., Qin, H., Zhang, L., Liu, X., Huang, S., Hu, J., & Jiang, M. (2005). Electrical and CO gas-sensing properties of perovskite-type $La_{0.8}Pb_{0.2}Fe_{0.8}Co_{0.2}O_3$ semiconductive materials. *Physica B: Condensed Matter, 368*(1-4), 204-208.

Sun, L., Qin, H., Wang, K., Zhao, M., & Hu, J. (2011). Structure and electrical properties of nanocrystalline $La_{1-x}Ba_xFeO_3$ for gas sensing application. *Materials Chemistry and Physics, 125*(1-2), 305-308.

Tawichai, N., Sittiyot, W., Eitssayeam, S., Pengpat, K., Tunkasiri, T., & Rujijanagul, G. (2012). Preparation and dielectric properties of barium iron niobate by molten-salt synthesis. *Ceramics International, 38*, S121-S124.

Zhang, K., & Fredkin, D. R. (1999). Effects of partial surface anisotropy on a fine magnetic particle. *Journal of applied physics, 85*(8), 6187-6189.